Scientific Research Publishing

Advances in Nanoparticles, 2025, 14(4), 142-157
https://www.scirp.org/journal/anp
ISSN Online: 2169-0529
ISSN Print: 2169-0510

Adsorption of Methylene Blue from Water Solution on Mesoporous Pseudoboehmite (*γ-AlOOH*) Synthesized Via a Mineral Route

Idriss Mahamat Yaya[1*], Djonbe Tchonnon Valery[1], Ech-chahad Abdellah[2]

[1]Département de Chimie, University of N'Djamena—Laboratoire de l'Eau et de l'Environnement, N'Djamena, Chad
[2]Laboratory of Applied Chemistry and Environment, Faculty of Science and Technology, University Hassan I, Settat, Morocco
Email: *idrisschagrami@gmail.com

How to cite this paper: Yaya, I.M., Valery, D.T. and Abdellah, E. (2025) Adsorption of Methylene Blue from Water Solution on Mesoporous Pseudoboehmite (*γ-AlOOH*) Synthesized via a Mineral Route. *Advances in Nanoparticles*, **14**, 142-157.
https://doi.org/10.4236/anp.2025.144009

Received: September 1, 2025
Accepted: October 28, 2025
Published: October 31, 2025

Abstract

In this study, pseudoboehmite (nano-boehmite) synthesized by A Route Mineral used to adsorb of methylene blue dye solution. The effect of experimental parameters pH, contact time, temperature and initial concentration were studied on adsorption. Results indicated that the optimal pH for adsorption is 10, with the experiments conducted at a temperature of 25˚C and adsorption reaches equilibrium after 30 minutes. The optimum adsorbent amount is 0.03 g. The equilibrium data were perfectly represented by the Freundlich isotherm and the adsorption behavior can be better described by pseudo-second-order model.

Keywords

Pseudoboehmite, Adsorption, Methylene Blue

1. Introduction

Water, the source of all life, is extensively used in various industries such as textiles, dyeing, paper manufacturing, beverages, food processing, cosmetics, leather tanning, plastics, detergents, and others. These industries, which rely on synthetic dyes, generate wastewater of varying volumes and chemical compositions due to the diversity of dyes used and production methods employed [1]. This wastewater is generally toxic, resistant to biodegradation, and persistent in the environment, contaminating not only surface waters but also underground water reservoirs [2] [3]. The pretreatment of industrial wastewater is a critical concern that must be addressed before it can be safely discharged from industrial sites. It is also im-

portant to note that the presence of these dyes, even at very low concentrations in drinking water, can cause adverse health effects in both humans and animals [4] [5]. Moreover, the discharge of colored wastewater produced by these industries into aquatic environments reduces sunlight penetration and visibility, leading to eutrophication and disturbances in aquatic ecology. This phenomenon not only impairs the intensity of photosynthesis in aquatic plants and algae but also contributes to environmental degradation [1] [6]-[8]. Various techniques have been employed to remove dyes from industrial effluents, including chemical oxidation, membrane separation, coagulation/flocculation, and ion exchange [9]-[11]. Unfortunately, most of these methods are expensive, require large quantities of materials, and are not environmentally sustainable. Biological treatment, which utilizes both living and non-living biomass for dye decolorization, offers a cost-effective and eco-friendly alternative [12]-[14]. A wide range of materials—such as zeolites, clays, activated carbon, polymers, eggshell particles, etc. have been reported to exhibit dye adsorption capabilities [15]-[20]. However, these materials have limitations, including low dye removal efficiency [21] and the transfer of dyes from the liquid to the solid phase. Despite these drawbacks, adsorption remains the most promising decolorization technique due to its simple implementation, high efficiency with appropriate adsorbents, and economic viability [22]. Nanometer- and micrometer-sized materials present interesting opportunities for the complete removal of organic dyes such as methylene blue (MB) from wastewater. Their small size and high specific surface area enables them to function effectively as filtration supports and catalysts [23]-[25]. To date, extensive research has focused on these materials in various morphologies particles, spheres, sheets, rods, tubes, and spikes—each offering potential for diverse applications [26]-[28]. Precipitation is an easy, straightforward, and cost-effective method for synthesizing nanoparticles and their composites, particularly when the solvent used can be recycled. Boehmite (*γ-AlOOH*) and its oxide derivatives, such as *α*-Al_2O_3 and *γ*-Al_2O_3, are among the nanostructures receiving considerable attention. These materials have been extensively studied for applications in catalysis, adsorption, flame retardancy, and optics [29]. To date, several types of boehmite nanostructures—such as nanorods, nanotubes [30], nanofibers [31], and nanowires [32] have been identified, each possessing unique physical and chemical properties. The aim of this study is to evaluate the dye removal efficiency of pseudoboehmite (*γ-AlOOH*), synthesized through an inorganic route, for the adsorption of cationic dyes under varying conditions, including contact time, pH, initial dye concentration, and temperature. Adsorption kinetics, isotherm models, and thermodynamic parameters were considered to describe the dye adsorption processes.

2. Materials and Methods

2.1. Materials

The products and materials used in this study include:

- The adsorbate: methylene blue (MB), a cationic dye with CI index 52015, mo-

lecular formula $C_{16}H_{18}N_3SCl$, and a molar mass of 319.85 g/mol.

- The adsorbent: Mesoporous Pseudoboehmite (*γ-AlOOH*) synthesized via a mineral route. This boehmite has a specific surface area of 317.29 m^2/g, an average pore diameter of 4.7353 nm, and a pore volume of 0.385085 cm^3/g. **Figure 1** shows the X-ray diffraction (XRD) pattern of the boehmite [33].
- All aqueous solutions were prepared in distilled water, and pH adjustments were made using sodium hydroxide NaOH (0.1 M) (98%) and hydrochloric acid HCl (0.1 M) (37%); 98% and 37% are the percentages of the pure reagents.
- UV-Vis absorption spectrum: UV-vis absorption spectra were acquired on a Cary 100 UV-vis spectrometer (Varian, USA) at room température (23˚C - 25˚C) and using a double beam. The pH metre: A Metrohm 692 pH meter (Herisau, Switzerland).

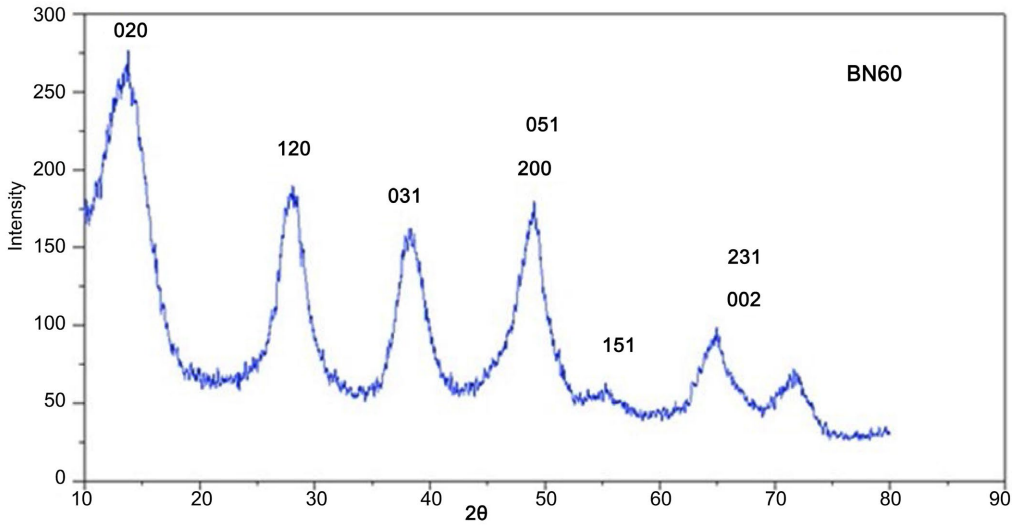

Figure 1. Diffractogramme DRX of pseudoboehmite.

2.2. Method

Batch Studies on the Adsorption of MB onto *γ-AlOOH*:

Adsorption tests were carried out in batch mode under varying initial conditions of pH, temperature, and dye concentration. In the experiment, beakers containing a fixed mass of adsorbent (30 mg) were filled with 50 mL of the dye solution (30 $mg{\cdot}L^{-1}$). The beakers, adjusted to the required pH, were subjected to continuous stirring for 180 min at 25˚C using a multi-station shaker. The absorbance of the filtrates was measured using a UV-visible spectrophotometer at the wavelength corresponding to the maximum absorbance of the sample ($\lambda = 664$ nm). The adsorption capacity of methylene blue and the removal efficiency, which indicates the exact rate of MB elimination by boehmite, were calculated using Equation (1) and Equation (2), respectively:

$$q_e = (c_o - c_e) \times v/m \quad (1)$$

$$R = (c_o - c_e)/c_o \times 100 \quad (2)$$

q_e: Equilibrium adsorption capacity ($mg \cdot g^{-1}$).
C_o: Dye's initial concentration ($mg \cdot L^{-1}$).
C_e: Dye's equilibrium concentration ($mg \cdot L^{-1}$).
m: Adsorbant mass (g).
V: Dye's solution volume (L).

2.2.1. Sorption Isotherms

To determine the adsorption isotherms at 25˚C, we used the batch equilibration method. Then, 30 mg of adsorbent was added to 50 mL of dye solution, at concentrations ranging from 50 to 500 $mg \cdot L^{-1}$; the system was allowed to reach equilibrium by maintaining a contact time of 24 h. The resulting experimental data were fitted to Langmuir (Equation (3)) and Freundlich (Equation (4)) isotherm models. The parameters obtained from isotherm modeling provide important insights into the adsorption mechanism, surface properties, and adsorbent-adsorbate affinities. Among the various models, we selected the two most significant: the Langmuir model and the Freundlich model. The Langmuir model is particularly useful for describing the monomolecular adsorption of a solute, forming a monolayer on the surface of an adsorbent. This model applies when the adsorbed species are fixed to well-defined, homogeneous sites, with each site capable of binding only one molecule. The adsorption energy is assumed to be identical for all sites and independent of the presence of other adsorbed species on neighboring sites. The empirical Freundlich model is based on adsorption onto heterogeneous surfaces, where the adsorption sites possess varying affinities and energies. Unlike the Langmuir model, which assumes uniform surface and monolayer adsorption, the Freundlich model accounts for multilayer adsorption and is particularly suitable for describing non-ideal and reversible adsorption processes on heterogeneous surfaces. It is commonly used to represent systems where the surface of the adsorbent is energetically non-uniform.

$$\frac{1}{q_e} = \frac{1}{q_m} + \frac{1}{k_1 \times q_m} \times \frac{1}{c_e} \tag{3}$$

K_L is the Langmuir equilibrium constant ($L \cdot mg^{-1}$), q_m represents the maximum adsorption capacity of the adsorbent to form a monolayer ($mg \cdot g^{-1}$), while q_e ($mg \cdot g^{-1}$) denotes the amount of dye adsorbed at equilibrium.

$$\ln q_e = \ln k_f = \frac{1}{n} \ln c_e \tag{4}$$

The Freundlich constants, K_F ($mg \cdot g^{-1}$) and n, are associated with the adsorption capacity and intensity of the adsorbent, respectively. Slope $1/n$ is a measure of the surface heterogeneity.

2.2.2. Kinetics Studies

Kinetic modeling is essential to understand the rate-controlling steps and mechanisms involved in the adsorption process. Three commonly applied models are the pseudo-first-order and pseudo-second-order, models [34].

- **Pseudo-First-Order Model (Lagergren model)**

This model assumes that the rate of occupation of adsorption sites is proportional to the number of unoccupied sites.

$$\ln\left(q_e - q_t\right) = \ln q_e - k_1 \cdot t \tag{5}$$

- **Pseudo-Second-Order Model:**

This model assumes that adsorption follows second-order kinetics and may involve chemisorption as the rate-limiting step.

$$1/q_t = 1/K_2 \cdot q_{e2} + \left(1/q_e\right) \cdot t \tag{6}$$

q_t: Adsorbed dye at time t ($mg \cdot g^{-1}$); q_e: Equilibrium adsorbed dye ($mg \cdot g^{-1}$); k_1 (min^{-1}) and k_2 ($g \cdot mg^{-1} \cdot min^{-1}$): Equilibrium rate constant characteristics of the pseudo-first-order and pseudo-second-order models, respectively.

3. Results and Discussions

3.1. Effect of pH

To investigate the effect of pH on the adsorption effeiciency of the dye, 0.03 g of the adsorbent was introduced into 50 mL of methylene blue (MB) solution at a concentration of 30 $mg \cdot L^{-1}$. The influence of pH variation on the amount adsorbed was studied over a pH range from 3 to 12. The pH values were adjusted using acidic (HCl) or alkaline (NaOH) solutions and maintained during the equilibrium period. Pseudoboehmite contains surface functional groups (OH^-) that can undergo protonation in acidic media to form $-OH_2^+$ groups, resulting in a positively charged surface. In basic media, these hydroxyl groups can be deprotonated to form $-O^-$ groups, creating a negatively charged surface. At highly acidic pH values, the large number of protons in the solution compete with MB^+ for access to the active adsorption sites, thereby reducing the extent of MB-adsorbent complexation. Additionally, the electrostatic repulsion between MB cations and the positively charged adsorbent surface at $pH < pH_{pzc}$ hinders effective adsorption. It should be noted that the point of zero charge (pH_{pzc}) is defined, as the pH at which the net surface charge of an adsorbent becomes zero, is an important physico-chemical parameter providing information on the phenomena occurring at the surface of adsorbents. At a pH below pHpzc, protonated adsorbent surface functional groups attract negatively charged adsorbates due to an excess H^+. At a pH above pH_{pzc}, the positively charged adsorbates are adsorbed onto the negatively charged adsorbent surface. Therefore, strongly acidic conditions are not favorable for the removal of MB using the proposed adsorbent. As the pH increases, these effects are mitigated, leading to improved dye removal efficiency. At higher pH values ($pH \geq pH_{pzc}$), the adsorbent surface becomes negatively charged, promoting stronger electrostatic attraction with the positively charged MB^+ molecules and resulting in enhanced adsorption [11] [35] [36]. Based on this, we focused on pH values equal to or above 7, particularly since methylene blue (MB^+) remains positively charged (cationic) in basic media. The optimal pH was determined to be 10, at which the maximum

removal efficiency of MB reached 89.07%, Figure 2.

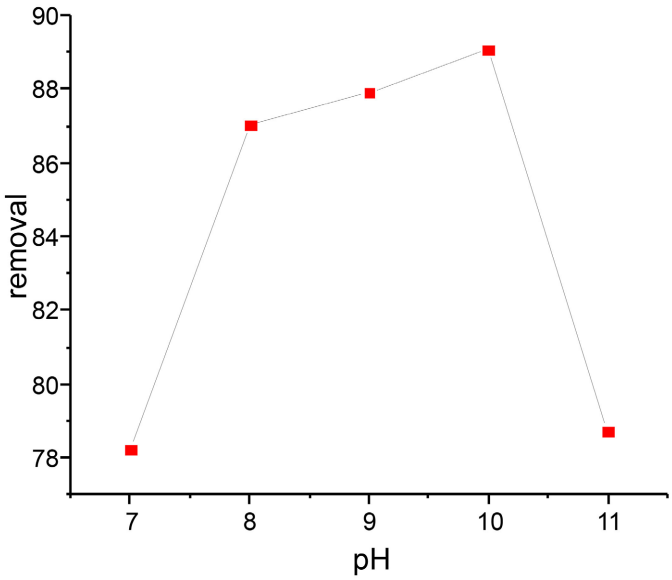

Figure 2. Effect of pH on the efficiency of removing MB by *γ-AlOOH*.

3.2. The Effect of Adsorbent Amount

To investigate the effect of adsorbent dosage on dye removal, varying masses of adsorbent ranging from 10 mg to 80 mg were each added to 50 mL of methylene blue (MB) solution at a concentration of 30 mg·L^{-1}. As shown in Figure 3, the percentage of MB removal increased with increasing adsorbent mass. This behavior is attributed to the greater number of available adsorption sites provided by the increased quantity of adsorbent, thereby enhancing the amount of dye adsorbed. Above 30 mg, the system reached equilibrium, and no significant increase in removal efficiency was observed with further increases in adsorbent mass. Therefore, subsequent experiments were conducted using this optimal dosage of 30 mg, Figure 3.

3.3. The Effect of MB Dye

At various initial concentrations of methylene blue (ranging from 10 to 80 mg·L^{-1}), the optimal adsorbent dosage and pH were maintained. As shown by the adsorption curve, a significant removal efficiency of MB was observed at concentrations between 10 and 30 mg·L^{-1}, reaching up to 90%. Beyond this range, the curve tends to stabilize. This phenomenon can be explained as follows: at lower dye concentrations, a large number of available pores and active sites on the surface of the adsorbent facilitate efficient adsorption. However, as the initial concentration of MB increases, these sites gradually become saturated due to the accumulation of dye molecules, leading to a decrease in removal efficiency. At a concentration of 90 mg·L^{-1}, the removal efficiency dropped to 53.073%, indicating that the adsorption capacity of the boehmite had reached near saturation, Figure 4.

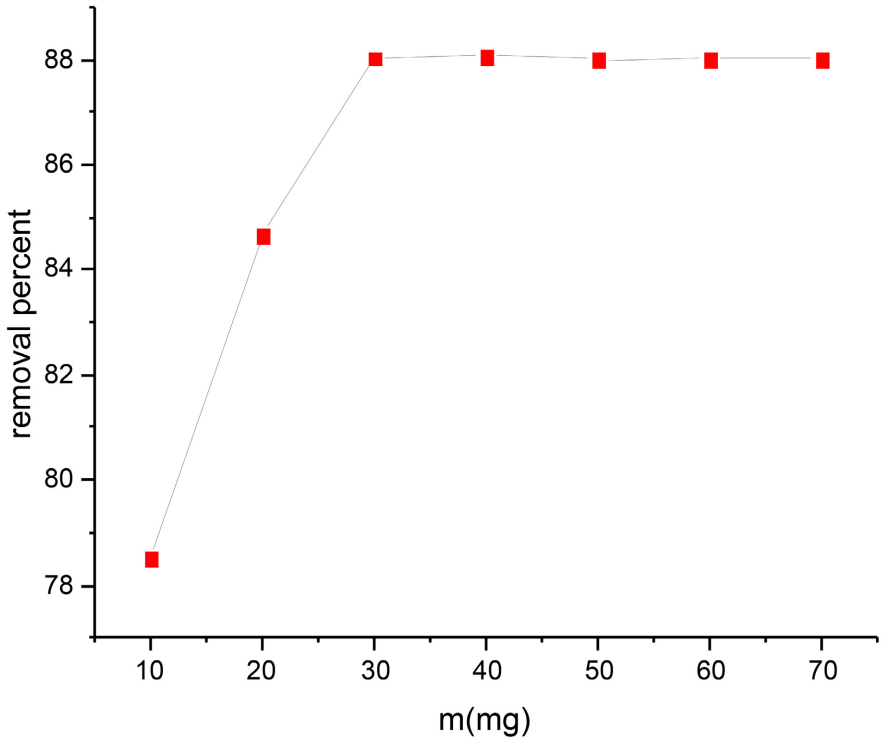

Figure 3. Effect of adsorbent initial mass (*γ-AlOOH*) on the efficiency of removing MB.

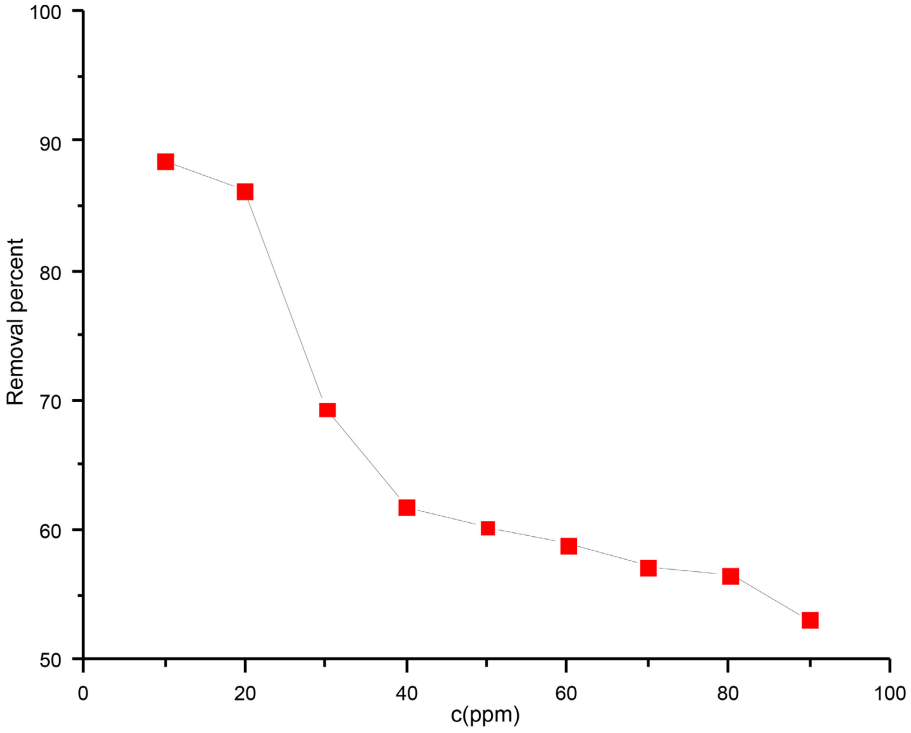

Figure 4. Effect of initial dye concentration on adsorption of MB.

3.4. The Effect of Adsorption Time

Kinetic studies aim to determine the sufficient and necessary time required to reach

adsorption equilibrium or maximum adsorption capacity. In the case of methylene blue (MB), the adsorption process was found to be rapid and increased progressively with contact time. In our study, equilibrium was reached after 30 minutes of contact. The high availability of active sites on the surface of the adsorbent is responsible for this rapid initial adsorption of MB from the aqueous solution during the first few minutes. Beyond this point, the amount of dye adsorbed remained nearly constant, even with extended contact time up to 180 minutes, indicating that equilibrium had been attained. The effect of contact time on MB adsorption by pseudoboehmite (*γ-AlOOH*). MB adsorption follows rapid kinetics, reaching a near-equilibrium state after 30 min, Figure 5. This could be justified by the availability of active sites.

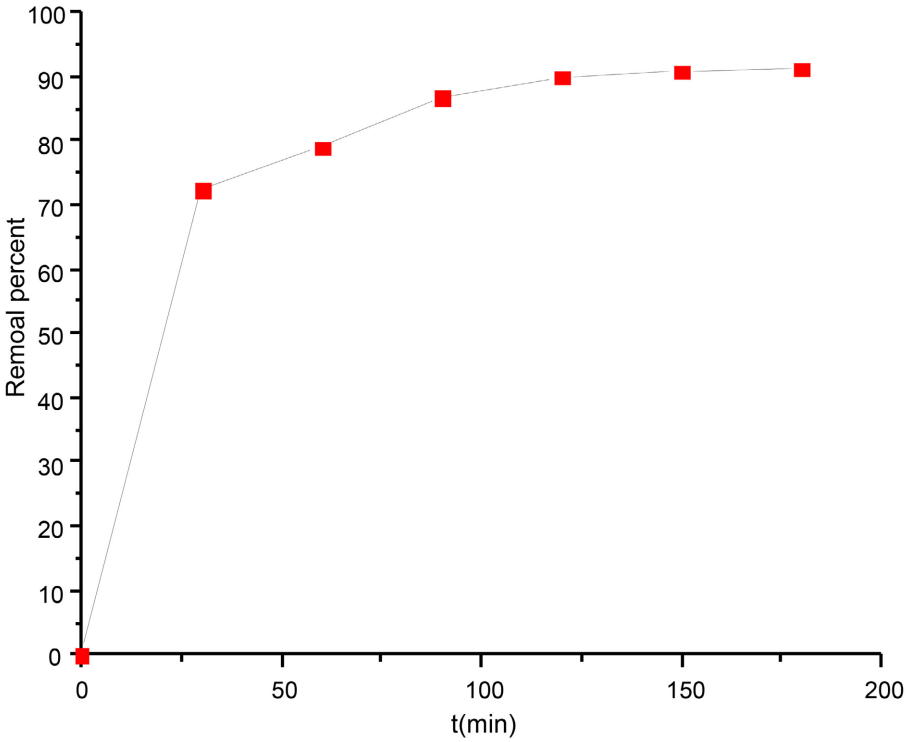

Figure 5. Effect of contact time on the adsorption of MB onto boehmite (*γ-AlOOH*).

3.5. The Effect Temperature

Similarly, the effect of temperature was studied using a thermostatic system at different temperatures (25˚C, 30˚C, 35˚C, and 60˚C), with absorbance readings taken at each condition. It was observed that increasing the temperature led to a decrease in removal efficiency, indicating a reversal of the adsorption process—desorption. This behavior suggests that the adsorption of methylene blue onto pseudoboehmite is an exothermic process. The observed desorption at higher temperatures is also advantageous for the regeneration of the adsorbent, allowing reuse in subsequent cycles. The optimal temperature for this experiment was found to be 25˚C, as the highest amount of MB was adsorbed at this ambient condition, Figure 6.

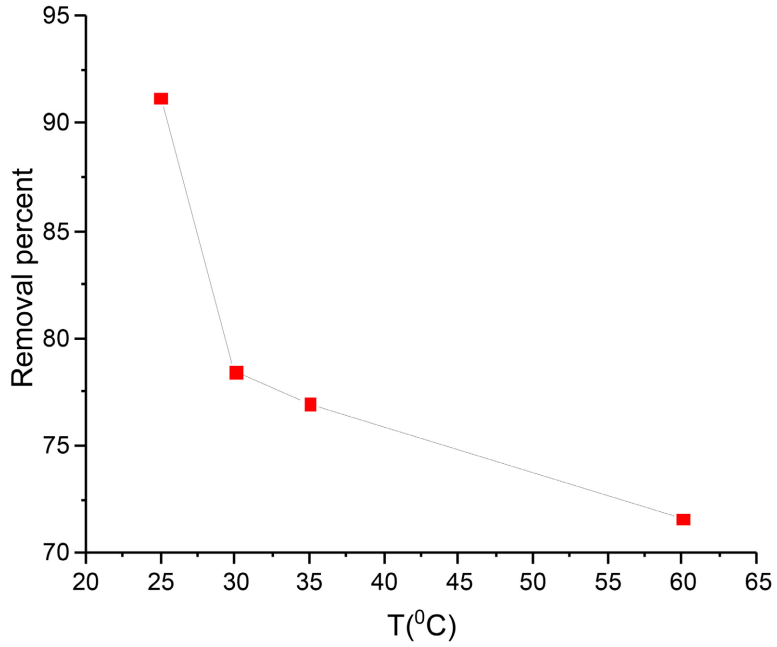

Figure 6. Effect of temperature on the adsorption of MB onto boehmite (*γ-AlOOH*).

3.6. Kinetic Studies

Two models, including the pseudo-first-order and the pseudo-second-order (**Figure 7** and **Figure 8**), were used to adjust the experimental data. The pseudo-second-order model has a correlation coefficient ($\mathbf{R^2 = 0.997}$) higher than the value obtained for the pseudo-first-order model ($\mathbf{R^2 = 0.791}$). This indicates that the pseudo-second-order model best describes the adsorption data. The pseudo-second-order kinetic model fitted well with all experimental data, meaning that the adsorption rate was mainly determined by the chemical adsorption process. This fitting result indicated that the electron transfer, exchange, or sharing was generated, and chemical bond was formed in the adsorption process. The k_1 and k_2 are presented in **Table 1** [11] [37]-[40].

3.7. The Equilibrium Studies

The adjustment of the experimental data to the Langmuir and Freundlich models is shown in **Figure 9** and **Figure 10**. The Freundlich model is considered most appropriate because it provides a better fit with the highest ($\mathbf{R^2 = 0.85}$) compared to the Langmuir isotherm, which had a correlation coefficient of about **0.81** (**Table 2**). However, the intrinsic parameters of Langmuir isotherm have a negative value. These negative values of Q_{max} and K_L are attributed more to the properties of the adsorbent than to the experimental conditions. Specific characteristics of the adsorbent, such as the presence of heterogeneous surface sites or complex interactions between adsorbed molecules, can render the Langmuir model unsuitable. Perwitasari *et al.* reported that, for the Langmuir equation, all linearized plots yield negative values of K_L and Q_{max}; consequently, the adsorption process is better suited to a heterogeneous surface [41]. Indeed, our adsorbent is a material with a

heterogeneous surface [33]. The Freundlich isotherm was all better than the Langmuir isotherm, implying that the adsorption process involved multimolecular layers of coverage, and heterogeneous nature of adsorptive sites on the surface of adsorbent [1] [42]. The Langmuir and Freundlich constants for the adsorption isotherm models and statistical are summarized in **Table 2**. The intensity factor was found higher to unity ($1/n = 1.39$) which corresponded to a favourable adsorption [43].

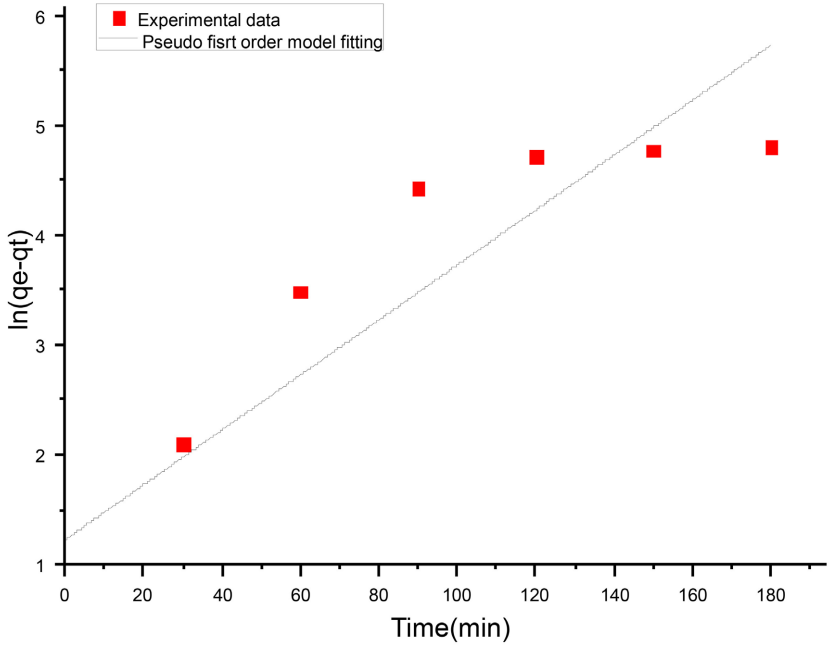

Figure 7. Plots of the pseudo-first-order.

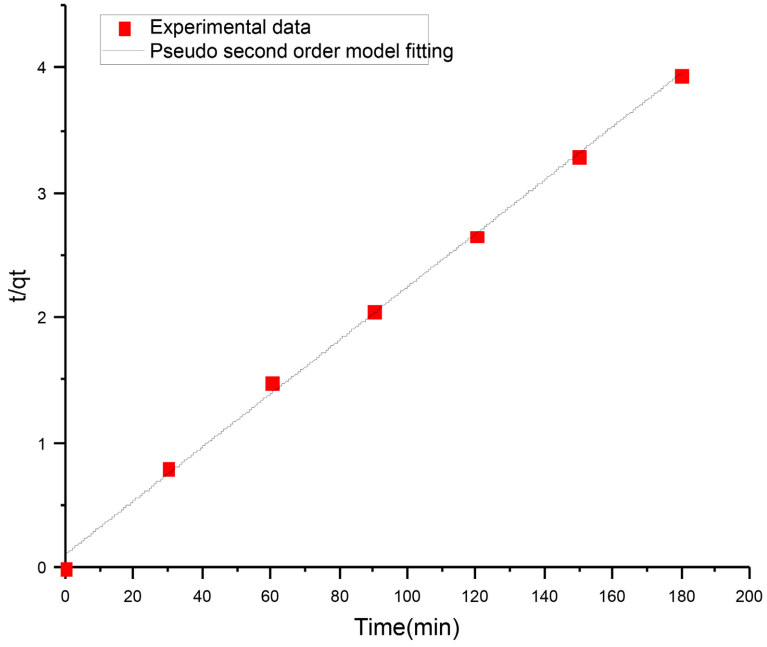

Figure 8. Plot of the pseudo-second order.

Table 1. Chemical bond formed in the adsorption process.

Order	Pseudo-first order	Pseudo-second order
R^2	0.79	0.99783
K	0.00014	0.0043
q_e	3.40	46.75

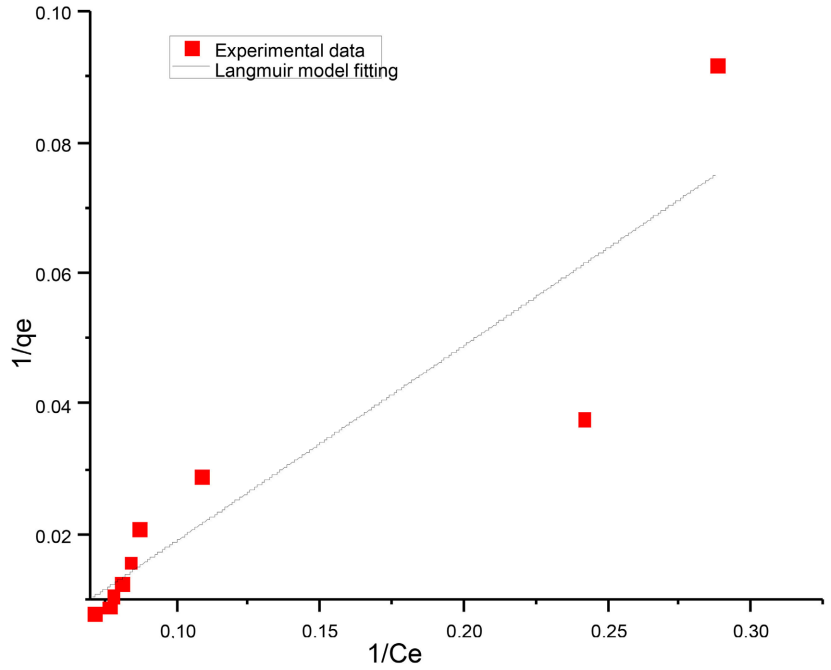

Figure 9. Langmuir model.

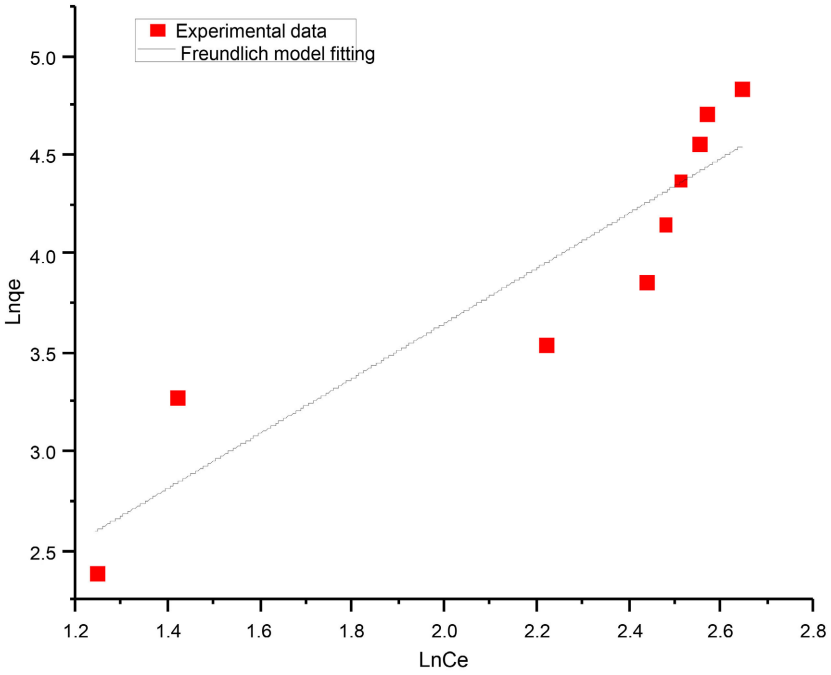

Figure 10. Freundlich model.

Table 2. The Langmuir and Freundlich constants for the adsorption isotherm models.

Langmuir isotherm				Freundlich isotherm			
R^2	K_L (l/mg)	Q_{max} (mg/g)	R_L	R^2	$1/n$	n	K_f
0.81	−0.036	−91.99	1.00	0.85	1.39	0.72	7.26

3.8. Thermodynamic Studies

The Gibb's free energy (ΔG^0), entropy (ΔS^0), and enthalpy (ΔH^0) changes for the adsorption were determined by:

$$\ln k_l = \left(\Delta S^0\right)/R - \left(\Delta H^0\right)/RT \tag{7}$$

$$\Delta G^0 = \Delta H^0 - T\Delta S^0 \tag{8}$$

where T is the solution temperature (K), R is the universal gas constant (8.314 $J{\cdot}K^{-1}{\cdot}mol^{-1}$) and K_l is the equilibrium constant. The calculated thermodynamic parameters are demonstrated in Table 3. The values of Gibbs free energy ΔG^0 had been calculated by knowing the ΔH^0 and the ΔS^0 and ΔH^0 were obtained from a plot of $\ln K_l$ versus $1/T$, from Equation (7). Once these two parameters were obtained, ΔG^0 is determined from Equation (8). The respective values of thermodynamic parameters for adsorption of methylene blue using pseudoboehmite are given in Table 3. The negative values of the free energy change (ΔG^0) indicate that the adsorption of methylene blue is favorable and spontaneous process. The negative value of change in enthalpy (ΔH^0) indicates the exothermic nature of adsorption process. The negative entropy (ΔS^0) value of entropy change indicated a more ordered distribution of Methylene Blue solution in solid phase rather than in liquid phase [1] (Figure 11).

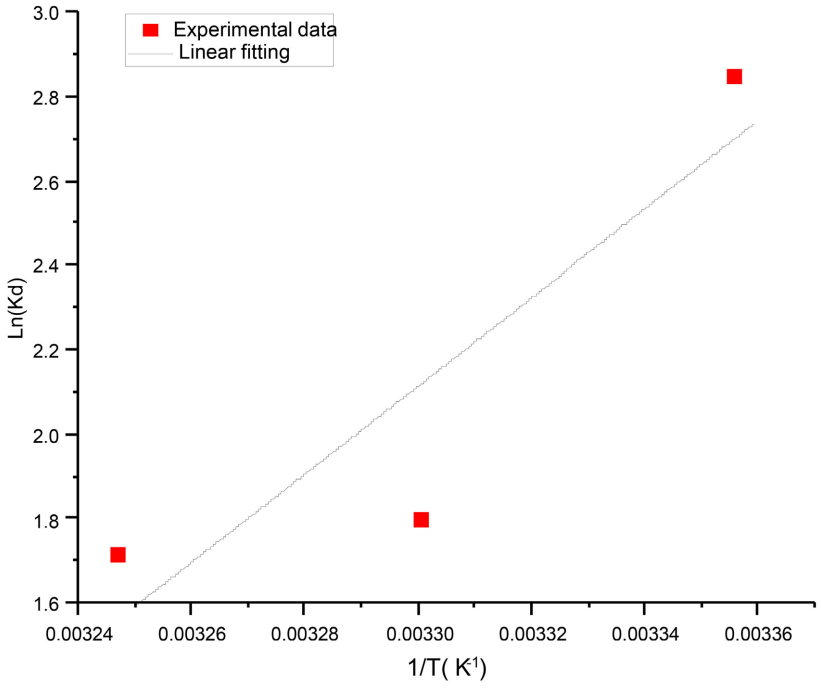

Figure 11. Plot of lnkd vs. $1/T$ for the adsorption of BM onto Pseudoboehmite.

Table 3. Thermodynamic parameters.

Adsorbant	T (K)	ΔG^0 (KJ/mol)	ΔH^0 (KJ/mol)	ΔS^0 (KJ/mol)
	298	−7.05709549	−86.6984793	−0.26854062
	303	−4.53876283		
	308	−4.39775412		

4. Conclusion

The adsorption capacity of *γ-AlOOH* particles was evaluated for MB dye removal. Adsorbent shows promising adsorption capacitie for MB. Investigation of the isotherms revealed a close correlation with the Freundlich isotherm model. However, both models can also be applied under specific conditions. The kinetic data are in good agreement with the pseudo-second-order kinetic model. The efficiency of methylene blue removal increases as the temperature decreases. The negative enthalpy change (ΔH^0) further corroborates the exothermic nature of the adsorption process. Hence, pseudoboehmite can be regarded as a highly promising material for wastewater remediation.

Acknowledgements

Authors acknowledge the Universities Université de Ndjamena (Tchad) et Université Hassan 1er de Settat (Maroc).

Conflicts of Interest

The authors declare no conflicts of interest regarding the publication of this paper.

References

[1] Salimi, F., Emami, S.S. and Karami, C. (2017) Removal of Methylene Blue from Water Solution by Modified Nano-Boehmite with Bismuth. *Inorganic and Nano-Metal Chemistry*, **48**, 31-40. https://doi.org/10.1080/24701556.2017.1357628

[2] Rane, N.R., Chandanshive, V.V., Khandare, R.V., Gholave, A.R., Yadav, S.R. and Govindwar, S.P. (2014) Green Remediation of Textile Dyes Containing Wastewater by *Ipomoea hederifolia* L. *RSC Advances*, **4**, 36623-36632. https://doi.org/10.1039/c4ra06840h

[3] Wu, Y., Chen, L., Long, X., Zhang, X., Pan, B. and Qian, J. (2018) Multi-Functional Magnetic Water Purifier for Disinfection and Removal of Dyes and Metal Ions with Superior Reusability. *Journal of Hazardous Materials*, **347**, 160-167. https://doi.org/10.1016/j.jhazmat.2017.12.037

[4] Ai, L., Zhang, C., Liao, F., Wang, Y., Li, M., Meng, L., *et al.* (2011) Removal of Methylene Blue from Aqueous Solution with Magnetite Loaded Multi-Wall Carbon Nanotube: Kinetic, Isotherm and Mechanism Analysis. *Journal of Hazardous Materials*, **198**, 282-290. https://doi.org/10.1016/j.jhazmat.2011.10.041

[5] Kamaria, M., Shafieea, S., Salimia, F. and Karami, C. (2019) Comparison of Modified Boehmite Nanoplatelets and Nanowires for Dye Removal from Aqueous Solution. *Desalination and Water Treatment*, **161**, 304-314.

[6] Pearce, C. (2003) The Removal of Colour from Textile Wastewater Using Whole Bac-

terial Cells: A Review. *Dyes and Pigments*, **58**, 179-196. https://doi.org/10.1016/s0143-7208(03)00064-0

[7] Arslan, İ., Balcioğlu, I.A. and Bahnemann, D.W. (2000) Advanced Chemical Oxidation of Reactive Dyes in Simulated Dyehouse Effluents by Ferrioxalate-Fenton/UV-A and TiO2/UV-A Processes. *Dyes and Pigments*, **47**, 207-218. https://doi.org/10.1016/s0143-7208(00)00082-6

[8] Sauer, T., Neto, G.C., Jose, H. and Moreira, R. (2002) Kinetics of Photocatalytic Degradation of Reactivedyes in a TiO2 Slurry Reactor. *Journal of Photochemistry and Photobiology A*: *Chemistry*, **149**, 147-154.

[9] Srinivasan, A. and Viraraghavan, T. (2010) Decolorization of Dye Wastewaters by Biosorbents: A Review. *Journal of Environmental Management*, **91**, 1915-1929. https://doi.org/10.1016/j.jenvman.2010.05.003

[10] Ben Younes, S., Bouallagui, Z. and Sayadi, S. (2012) Catalytic Behavior and Detoxifying Ability of an Atypical Homotrimeric Laccase from the Thermophilic Strain Scytalidium Thermophilum on Selected Azo and Triarylmethane Dyes. *Journal of Molecular Catalysis B*: *Enzymatic*, **79**, 41-48. https://doi.org/10.1016/j.molcatb.2012.03.017

[11] Salimi, F., Rahimi, H. and Karami, C. (2019) Removal of Methylene Blue from Water Solution by Modified Nanogoethite by Cu. *Desalination and Water Treatment*, **137**, 334-344. https://doi.org/10.5004/dwt.2019.22922

[12] Yagub, M.T., Sen, T.K., Afroze, S. and Ang, H.M. (2014) Dye and Its Removal from Aqueous Solution by Adsorption: A Review. *Advances in Colloid and Interface Science*, **209**, 172-184. https://doi.org/10.1016/j.cis.2014.04.002

[13] Park, C., Lee, M., Lee, B., Kim, S., Chase, H.A., Lee, J., *et al.* (2007) Biodegradation and Biosorption for Decolorization of Synthetic Dyes by Funalia Trogii. *Biochemical Engineering Journal*, **36**, 59-65. https://doi.org/10.1016/j.bej.2006.06.007

[14] Taha, M., Adetutu, E.M., Shahsavari, E., Smith, A.T. and Ball, A.S. (2014) Azo and Anthraquinone Dye Mixture Decolourization at Elevated Temperature and Concentration by a Newly Isolated Thermophilic Fungus, Thermomucor Indicae-Seudaticae. *Journal of Environmental Chemical Engineering*, **2**, 415-423. https://doi.org/10.1016/j.jece.2014.01.015

[15] Cornell, R. and Schwertmann, U. (2003) Dissolution, the Iron Oxides: Structure, Properties, Reactions, Occurrences and Uses. 2nd Edition, Wiley-VCH, 297-344.

[16] Senthil Kumar, P., Sivaranjanee, R., Vinothini, U., Raghavi, M., Rajasekar, K. and Ramakrishnan, K. (2014) Adsorption of Dye onto Raw and Surface Modified Tamarind Seeds: Isotherms, Process Design, Kinetics and Mechanism. *Desalination and Water Treatment*, **52**, 2620-2633. https://doi.org/10.1080/19443994.2013.792016

[17] Kumar, P.S., Pavithra, J., Suriya, S., Ramesh, M. and Kumar, K.A. (2015) *Sargassum wightii*, a Marine Alga Is the Source for the Production of Algal Oil, Bio-Oil, and Application in the Dye Wastewater Treatment. *Desalination and Water Treatment*, **55**, 1342-1358. https://doi.org/10.1080/19443994.2014.924032

[18] Mathivanan, V., Geetha Manjari, S., Ineya, R., Saravanathamizhan, R., Senthil Kumar, P. and Ramakrishnan, K. (2016) Enhanced Photocatalytic Decolorization of Reactive Red by Sonocatalysis Using TiO2 Catalyst: Factorial Design of Experiments. *Desalination and Water Treatment*, **57**, 7120-7129. https://doi.org/10.1080/19443994.2014.983182

[19] Salimi, F., Eskandari, M. and Karami, C. (2017) Investigation of Methylene Blue Adsorption in Wastewater Using Nano-Zeolite Modified with Copper. *Desalination and Water Treatment*, **85**, 206-214. https://doi.org/10.5004/dwt.2017.21248

[20] Salimi, F., Tahmasobi, K., Karami, C. and Jahangiri, A. (2017) Preparation of Modified Nano-SiO2 by Bismuth and Iron as a Novel Remover of Methylene Blue from Water Solution. *Journal of the Mexican Chemical Society*, **61**, 250-259. https://doi.org/10.29356/jmcs.v61i3.351

[21] Alvarez, M., Rueda, E.H. and Sileo, E.E. (2007) Simultaneous Incorporation of Mn and Al in the Goethite Structure. *Geochimica et Cosmochimica Acta*, **71**, 1009-1020. https://doi.org/10.1016/j.gca.2006.11.012

[22] Crini, G., Lichtfouse, E., Wilson, L.D. and Morin-Crini, N. (2019) Conventional and Non-Conventional Adsorbents for Wastewater Treatment. *Environmental Chemistry Letters*, **17**, 195-213. https://doi.org/10.1007/s10311-018-0786-8

[23] AbdEl-Salam, A.H., Ewais, H.A. and Basaleh, A.S. (2017) Silver Nanoparticles Immobilised on the Activated Carbon as Efficient Adsorbent for Removal of Crystal Violet Dye from Aqueous Solutions. a Kinetic Study. *Journal of Molecular Liquids*, **248**, 833-841. https://doi.org/10.1016/j.molliq.2017.10.109

[24] Sadegh, H., Ali, G.A.M., Gupta, V.K., Makhlouf, A.S.H., Shahryari-ghoshekandi, R., Nadagouda, M.N., *et al.* (2017) The Role of Nanomaterials as Effective Adsorbents and Their Applications in Wastewater Treatment. *Journal of Nanostructure in Chemistry*, **7**, 1-14. https://doi.org/10.1007/s40097-017-0219-4

[25] Shinde, S.G. and Shrivastava, V.S. (2016) Synthesis of γ-Alumina (Al_2O_3) Nanoparticles and their Potential for Use as an Adsorbent in the Removal of Methylene Blue Dye from Industrial Wastewater. *Asian Journal of Chemical and Environmental Research*, **9**, 129-132.

[26] Arshadi, M., Mehravar, M., Amiri, M.J. and Faraji, A.R. (2015) Synthesis and Adsorption Characteristics of an Heterogenized Manganese Nanoadsorbent Towards Methyl Orange. *Journal of Colloid and Interface Science*, **440**, 189-197. https://doi.org/10.1016/j.jcis.2014.10.053

[27] Huang, Q., Liu, M., Chen, J., Wan, Q., Tian, J., Huang, L., *et al.* (2017) Facile Preparation of Mos2 Based Polymer Composites via Mussel Inspired Chemistry and Their High Efficiency for Removal of Organic Dyes. *Applied Surface Science*, **419**, 35-44. https://doi.org/10.1016/j.apsusc.2017.05.006

[28] Jiang, Y., Gong, J., Zeng, G., Ou, X., Chang, Y., Deng, C., *et al.* (2016) Magnetic Chitosan-Graphene Oxide Composite for Anti-Microbial and Dye Removal Applications. *International Journal of Biological Macromolecules*, **82**, 702-710. https://doi.org/10.1016/j.ijbiomac.2015.11.021

[29] Mishra, D., Anand, S., Panda, R.K. and Das, R.P. (2000) Hydrothermal Preparation and Characterization of Boehmites. *Materials Letters*, **42**, 38-45. https://doi.org/10.1016/s0167-577x(99)00156-1

[30] Hou, H., Xie, Y., Yang, Q., Guo, Q. and Tan, C. (2005) Preparation and Characterization of *γ-ALOOH* Nanotubes and Nanorods. *Nanotechnology*, **16**, 741-745. https://doi.org/10.1088/0957-4484/16/6/019

[31] Wierenga, A., Philipse, A.P., Lekkerkerker, H.N.W. and Boger, D.V. (1998) Aqueous Dispersions of Colloidal Boehmite: Structure, Dynamics, and Yield Stress of Rod Gels. *Langmuir*, **14**, 55-65. https://doi.org/10.1021/la970376z

[32] Zhang, J., Liu, S., Lin, J., Song, H., Luo, J., Elssfah, E.M., *et al.* (2006) Self-Assembly of Flowerlike ALOOH (Boehmite) 3D Nanoarchitectures. *The Journal of Physical Chemistry B*, **110**, 14249-14252. https://doi.org/10.1021/jp062105f

[33] Yaya, I.M., Guillaume, N. and Arkhis, M. (2018) The Synthesis of Mesoporous Pseudo Boehmite by a Route Mineral and Its Transformation into Alumina-γ. *Materials Science: An Indian Journal*, **16**, Article 140.

[34] Revellame, E.D., Fortela, D.L., Sharp, W., Hernandez, R. and Zappi, M.E. (2020) Adsorption Kinetic Modeling Using Pseudo-First Order and Pseudo-Second Order Rate Laws: A Review. *Cleaner Engineering and Technology*, **1**, Article 100032. https://doi.org/10.1016/j.clet.2020.100032

[35] Kamari, M., Shafiee, S., Salimi, F. and Karami, C. (2019) Comparison of Modified Boehmite Nanoplatelets and Nanowires for Dye Removal from Aqueous Solution. *Desalination and Water Treatment*, **161**, 304-314. https://doi.org/10.5004/dwt.2019.24295

[36] Wang, D., Li, Z., Lv, F., Guan, M., Chen, J., Wu, C., *et al.* (2023) Characterization of Microspheres *γ-ALOOH* and the Excellent Removal Efficiency of Congo Red. *Journal of Physics and Chemistry of Solids*, **174**, Article 111043. https://doi.org/10.1016/j.jpcs.2022.111043

[37] Sun, Y., Ding, C., Cheng, W. and Wang, X. (2014) Simultaneous Adsorption and Reduction of U(VI) on Reduced Graphene Oxide-Supported Nanoscale Zerovalent Iron. *Journal of Hazardous Materials*, **280**, 399-408. https://doi.org/10.1016/j.jhazmat.2014.08.023

[38] Khan, H., Iram, Gul, K., Ara, B., Khan, A., Ali, N., *et al.* (2020) Adsorptive Removal of Acrylic Acid from the Aqueous Environment Using Raw and Chemically Modified Alumina: Batch Adsorption, Kinetic, Equilibrium and Thermodynamic Studies. *Journal of Environmental Chemical Engineering*, **8**, Article 103927. https://doi.org/10.1016/j.jece.2020.103927

[39] Sheng, G., Li, J., Shao, D., Hu, J., Chen, C., Chen, Y., *et al.* (2010) Adsorption of Copper (II) on Multiwalled Carbon Nanotubes in the Absence and Presence of Humic or Fulvic Acids. *Journal of Hazardous Materials*, **178**, 333-340. https://doi.org/10.1016/j.jhazmat.2010.01.084

[40] Ciopec, M., Davidescu, C.M., Negrea, A., Grozav, I., Lupa, L., Negrea, P., *et al.* (2012) Adsorption Studies of Cr(iii) Ions from Aqueous Solutions by DEHPA Impregnated onto Amberlite XAD7—Factorial Design Analysis. *Chemical Engineering Research and Design*, **90**, 1660-1670. https://doi.org/10.1016/j.cherd.2012.01.016

[41] Perwitasari, D.S., Pracesa, Y.A.Y., Pangestu, M.A. and Tola, P.S. (2021) Langmuir and Freundlich Isotherm Approximation on Adsorption Mechanism of Chrome Waste by Using Tofu Dregs. 2*nd International Conference Eco-Innovation in Science*, *Engineering*, *and Technology*, Samara, 11 December 2021, 106-112. https://doi.org/10.11594/nstp.2021.1417

[42] Mve, M.Z., Mba, C.M.M., Eba, F. and Ondo, J.A. (2020) Study of the Adsorption Equilibrium of the Methylene blue from Aqueous Solution onto Activated Carbon of Coula Edulis Nut Shells. *Research Journal of Chemistry and Environment*, **24**, 40-50.

[43] Danesh, N., Hosseini, M., Ghorbani, M. and Marjani, A. (2016) Fabrication, Characterization and Physical Properties of a Novel Magnetite Graphene Oxide/Lauric Acid Nanoparticles Modified by Ethylenediaminetetraacetic Acid and Its Applications as an Adsorbent for the Removal of Pb(ii) Ions. *Synthetic Metals*, **220**, 508-523. https://doi.org/10.1016/j.synthmet.2016.07.025